ARTICLE IN PRESS

xxx (xxxx) xxx

Contents lists available at ScienceDirect

Biomaterials Advances

journal homepage: www.journals.elsevier.com/materials-science-and-engineering-c

Marine origin biomaterials using a compressive and absorption methodology as cell-laden hydrogel envisaging cartilage tissue engineering

Duarte Nuno Carvalho [a,b], David S. Williams [c], Carmen G. Sotelo [d], Ricardo I. Pérez-Martín [d], Andrew Mearns-Spragg [c], Rui L. Reis [a,b], Tiago H. Silva [a,b,*]

[a] 3B's Research Group, I3B's – Research Institute on Biomaterials, Biodegradables and Biomimetics of University of Minho, Headquarters of the European Institute of Excellence on Tissue Engineering and Regenerative Medicine, AvePark 4805-017, Barco, Guimarães, Portugal
[b] ICVS/3B's – PT Government Associate Laboratory, Braga/Guimarães, Portugal
[c] Jellagen Limited, Unit G6, Capital Business Park, Parkway, St Mellons, Cardiff CF3 2PY, United Kingdom
[d] Group of Food Biochemistry, Instituto de Investigaciones Marinas (IIM-CSIC), C/Eduardo Cabello 6, Vigo, Pontevedra, Spain

ARTICLE INFO

Keywords:
Marine biomaterials
Chondrocytes
Tissue-scaffolds
Biomedical engineering
Articular cartilage

ABSTRACT

In the recent decade, marine origin products have been growingly studied as building blocks complying with the constant demand of the biomedical sector regarding the development of new devices for Tissue Engineering and Regenerative Medicine (TERM). In this work, several combinations of marine collagen-chitosan-fucoidan hydrogel were formed using a newly developed eco-friendly compressive and absorption methodology to produce hydrogels (CAMPH), which consists of compacting the biopolymers solution while removing the excess of water. The hydrogel formulations were prepared by blending solutions of 5% collagen from jellyfish and/or 3% collagen from blue shark skin, with solutions of 3% chitosan from squid pens and solutions of 10% fucoidan from brown algae, at different ratios. The biopolymer physico-chemical characterization comprised Amino Acid analysis, ATR-FTIR, CD, SDS-PAGE, ICP, XRD, and the results suggested the shark/jellyfish collagen(s) conserved the triple helical structure and had similarities with type I and type II collagen, respectively. The studied collagens also contain a denaturation temperature of around 30–32 °C and a molecular weight between 120 and 125 kDa. Additionally, the hydrogel properties were determined by rheology, water uptake ability, degradation rate, and SEM, and the results showed that all formulations had interesting mechanical (strong viscoelastic character) and structural stability properties, with a significant positive highlight in the formulation of H_3 (blending all biopolymers, i.e., 5% collagen from jellyfish, 3% collagen from skin shark, 3% chitosan and 10% of fucoidan) in the degradation test, that shows a mass loss around 18% over the 30 days, while the H_1 and H_2, present a mass loss of around 35% and 44%, respectively. Additionally, the in vitro cellular assessments using chondrocyte cells (ATDC5) in encapsulated state revealed, for all hydrogel formulations, a non-cytotoxic behavior. Furthermore, Live/Dead assay and Phalloidin/DAPI staining, to assess the cytoskeletal organization, proved that the hydrogels can provide a suitable microenvironment for cell adhesion, viability, and proliferation, after being encapsulated. Overall, the results show that all marine collagen (jellyfish/shark)-chitosan-fucoidan hydrogel formulations provide a good structural architecture and microenvironment, highlighting the H_3 biomaterial due to containing more polymers in their composition, making it suitable for biomedical articular cartilage therapies.

Abbreviations: TERM, Tissue Engineering and Regenerative Medicine; CAMPH, Compressive and Absorption Methodology to Produce Hydrogels; jCOL, Jellyfish collagen; sCOL, Shark collagen; sCHT, Squid pen chitosan; aFUC, Algae Fucoidan; HA, Hyaluronic Acid; CS, Chondroitin Sulfate; H_1, Hydrogel 1 (composed by jCOL-sCHT-aFUC); H_2, Hydrogel 2 (composed by sCOL-sCHT-aFUC); H_3, Hydrogel 3 (composed by jCOL-sCOL-sCHT-aFUC); ECM, Extracellular Matrix; DD, Degree of Deacetylation; ATR-FTIR, Attenuated Total Reflectance – Fourier Transform InfraRed Spectroscopy; CD, Circular Dichroism; SDS-PAGE, Sodium Dodecyl Sulfate – Polyacrylamide Gel Electrophoresis; ICP, Inductively Coupled Plasma Spectrometer; XRD, X-ray Diffraction; SEM, Scanning Electron Microscopy; ATDC5, Chondrocyte cells.

* Corresponding author at: 3B's Research Group, I3B's – Research Institute on Biomaterials, Biodegradables and Biomimetics of University of Minho, Headquarters of the European Institute of Excellence on Tissue Engineering and Regenerative Medicine, AvePark 4805-017, Barco, Guimarães, Portugal.
E-mail address: tiago.silva@i3s.uminho.pt (T.H. Silva).

https://doi.org/10.1016/j.bioadv.2022.212843
Received 27 January 2022; Received in revised form 8 April 2022; Accepted 1 May 2022
Available online 5 May 2022

1. Introduction

Marine origin resources are an excellent natural alternative to mammal sources of materials and bioactive compounds since they can provide them in a sustainable form, to inspire the production of innovative biological devices for therapeutically approaches envisaging their application in tissue engineering and regenerative medicine (TERM). Moreover, it is claimed the lack of disease transmission risks, along with the absence of ethical reasons (social/religious) reinforcing the use of marine organisms for biomedicine [1–3].

In the recent decade, many of these marine materials, such as collagen, chitosan, and fucoidan, have been extensively studied by their similarities with proteins and polysaccharides present in the extracellular matrix (ECM) of humans, supporting the capacity to create new biomaterials that can mimic the composition of the native ECM, including in cartilage regions, due to constraints on self-repair capacity observed for this tissue [4,5]. For example, articular cartilage tissue contains a highly hydrated ECM, and it is composed mainly of type II collagen fibers (between 90 and 95%), glycosaminoglycans as hyaluronic acids (HA) and chondroitin sulfates (CS), and small molecular glycoproteins [6–8].

The marine collagen is a great candidate for TERM strategies considering the characteristic biological properties such as high biocompatibility, low antigenicity, non-toxicity, safe biodegradability [9], also it can provide appropriate signals that influence the cell adhesion, viability, proliferation, and migration [9–11]. Although chitosan is not present in mammal ECMs, it structurally shares a monomer with hyaluronic acid found especially in cartilage ECM [12]. That structural characteristic and the presence of remarkable natural properties such as biodegradability, biocompatibility, low toxicity, anti-inflammatory, and antibacterial, make the chitosan a great candidate for there use in cartilage tissue repair [13,14]. Similarly, fucoidan has the potential for this application due to its structural composition that resembles chondroitin sulfates, being both considered sulfated glycosaminoglycans [15]. Fucoidan can be found on the tissue wall of brown seaweeds and contains diverse biological effects, such as anticoagulant, anti-thrombotic, antiangiogenic, anti-inflammatory, antiviral, antioxidant, anti-tumoral, among others [16–18]. Additionally, it is known that these two types of glycosaminoglycans positively influence the proliferation and differentiation of chondrocytes cells [6]. Therefore, considering each polymer property, it is reasonable to expect that scaffolds prepared with collagen, chitosan, and fucoidan would potentially benefit cartilage restoration.

Recently, there has been a growing interest in constructing diverse scaffolds, for example, in the form of hydrogels, using one or more polymers according to several protocols for TERM approaches [19,20]. However, many of the proposed hydrogels required the use of chemical cross-linking agents, which may inadvertently contribute to toxicity if the non-reacted material is not properly removed and other strategies are being pursued to increase the physico-chemical properties of the resulting hydrogels and take advantage of their different biological properties for TERM [21]. Accordingly, we have recently proposed an innovative methodology [22] that allows the production of scaffolds in a fast and reproducible format, highlighting their eco-friendly character. The strategy consists of promoting ionic interactions between the polymers (natural crosslinking) at the same time that the residual liquid (solvents) is absorbed while a mild plastic compression occurs, resulting in a material with increased structural stability. Such a process is herein defined as a compressive and absorption methodology for the production of hydrogels (CAMPH). Moreover, it is known that natural electrostatic interactions have the advantage to typically elicit lower cell cytotoxicity when compared with chemical agents [23,24], thus promising application for cell encapsulation and 3D cell culture templates. In addition, the current societal concerns encompass obtaining alternative materials to those currently used in the biomedical sector, as well as developing optimized processes that assure a sustained, cost-effective process with a reduced environmental impact (i.e. solvent and material waste) [22,25].

The purpose of this study was to establish and expand the proposed CAMPH with the possibility to extend this methodology when using other sources. Moreover, it was also aimed to evaluate the potential of incorporating a step for cell encapsulation within the polymeric structure. Thus, a considerable process optimization was performed to make this procedure profitable, reproducible, and fast, i.e., accessing the 3R's (Reduce, Reuse and Recycle) policy, especially by using disposable materials (greener for the environment). For this, marine origin hydrogels were produced by CAMPH using different formulations of collagen-chitosan-fucoidan blends. The developed hydrogels were extensively characterized regarding their physico-chemical properties, such as composition, rheology behavior, water uptake ability, and degradability. Their cytotoxicity, as well as the capacity to support cell viability and proliferation, were also assessed, evaluating cell metabolic activity and morphological/cytoskeletal organization, aiming for a future application in cartilage tissue engineering.

2. Materials and methods

2.1. Materials

Collagen from jellyfish (*Rhizostoma pulmo*) (jCOL) was provided from Jellagen Pty Ltd. (UK), while collagen from blue shark (*Prionace glauca*) skin (sCOL) was extracted using the protocol described in [26]. Briefly, shark skins were treated with 0.1 M NaOH to remove the non-collagenous proteins and then treated with 0.5 M acetic acid to extract collagen, followed by dialysis, all performed in a cold room (3–5 °C) and finally freeze-dried. Fucoidan from brown algae (*Fucus vesiculosus*) (aFUC) was obtained from Marinova (Australia, product: Maritech® Fucoidan, FVF2011527), while chitosan was produced from squid pens of giant squid (*Dosidicus gigas*) (sCHT) according to the protocol used by Reys et al. [13], with a molecular weight of 348 kDa and a degree of deacetylation (DD) of 90.1% [27]. In brief, the squid chitin was deproteinized in 1 M NaOH at 80 °C for 22 h, and then the obtained chitin was converted into chitosan using a deacetylation method with the alkaline process (NaOH), at a ratio of 1:10 (w/v), under temperatures between 85 and 100 °C, over 2 h.

2.2. Characterization of the biopolymers

2.2.1. Amino acid analysis

The amino acid profile of collagen from jellyfish and blue sharks were determined by quantitative analysis using a Biochrome 30 (Biochrome Ltd., Cambridge, UK). Briefly, 5 mg/mL of jCOL and sCOL were completely hydrolyzed, and the resultant amino acids were separated by an ion-exchange column. After derivatization by ninhydrin, the obtained samples were analyzed at 570 nm. A standard of norleucine was used to determine the concentration of amino acids on the samples.

2.2.2. Circular dichroism (CD)

Circular dichroism (CD) measurements of jCOL and sCOL were analyzed using a Jasco Model J-1500 spectrometer and path length of 2 mm quartz cylindrical cuvette (Hellma, Germany). The cuvette was filled with 600 μL of 0.1 mg/mL of collagen in 50 mM acetic acid for each measurement. CD spectra were obtained by continuous wavelength scans (average of three scans) from 180 to 240 nm at a scan-rate of 50 nm/min, between 4 and 65 °C temperature range at a heating rate of 4 °C between measurements. For this, the ellipticity (Θ) of both collagen samples (jCOL and sCOL) and denaturation temperature was measured, and the results were fitted to the Boltzmann sigmoidal curve.

2.2.3. Attenuated Total Reflectance – Fourier Transform InfraRed (ATR–FTIR) spectroscopy

The ATR-FTIR spectra of the marine biopolymers were obtained in

transmission mode using a Shimadzu-IR Prestige 21 spectrometer equipped with attenuated total reflectance (ATR) crystal in the spectral region corresponding to 4000–600 cm^{-1} with a resolution of 2 cm^{-1} as the average of 32 individual scans.

2.2.4. Sodium Dodecyl Sulphate – Polyacrylamide Gel Electrophoresis (SDS-PAGE)

SDS-PAGE was prepared using reagents from Sigma SDS-PAGE reagents and cast on a Biorad Mini Protean II System. Freeze-dried collagens were dissolved with 0.5 M acetic acid at 5 mg/mL. The samples were heated for 10 min at 95 °C to denature the proteins completely, and 30 μL of each collagen sample was loaded in the gel. Also, 4 μL of protein marker (Page Ruler Prestained protein ladder 10 to 250 kDa) were loaded along with the samples. The electrophoresis was carried out at 90 V until the frontline reached the lower part of the gel. After running, the gel was stained with a Coomassie (0.125% Coomassie Blue R 250 (Biorad), 50% methanol and 10% acetic acid) staining solution for 40 min, then soaked 3 times on destaining solution (5% methanol and 7% acetic acid) during 30 min each and after that with distilled water overnight.

2.2.5. X-ray diffraction (XRD)

XRD measurements of jCOL and sCOL were performed using a conventional Bragg-Brentano diffractometer (Bruker D8 Advance DaVinci, Germany) equipped with CuKα radiation, at 40 kV and 40 mA. The data sets analysis was collected in the 2θ range of 5–50° with a step size of 0.02° and 1 s for each step. The average crystallite size was calculated using the Bragg equation (Eq. (1)), wherein $\lambda_{CuK\alpha} = 1.5406$:

$$d\ (\text{Å}) = \lambda/2\sin\theta \quad (1)$$

2.2.6. Inductively Coupled Plasma (ICP) spectrometer

The biopolymer solutions (1 mg/mL of jCOL, sCOL aFUC, or sCHT in 5% nitric acid) were analyzed by inductively coupled plasma atomic emission spectrometry (ICP AES) to evaluate principally if the marine source used contained any contamination due to the presence of heavy metals. The ICP analysis was performed on a JY 2000-2 spectrometer (HORIBA Jobin Yvon, USA). The absorption at specific wavelengths (λ = 422.67 nm for Ca, λ = 213.86 nm for Zn, λ = 279.55 nm for Mg, λ = 407.77 nm for Sr, λ = 766.49 nm for K, λ = 257.61 nm for Mn, λ = 214.91 nm for P, λ = 588.99 nm for Na, λ = 238.89 nm for Cu, λ = 259.94 nm for Fe, λ = 242.80 nm for Au), was measured. The concentrations were determined from standard calibration curves prepared using standard solutions with concentrations of 10 ppm, 5 ppm, 3 ppm, and 1 ppm. Additionally, some heavy metals as Al, As, Ag, Cd, Hg, and Pb, were analyzed by ICP-MS (Thermo Xseries), according to their isotopes (27, 75, 109, 111, 201, and 206 + 207 + 208, respectively). For this elementary determination, each sample was dissolved in a solution that contained 1 mL HNO_3, 2 mL H_2O_2, and 1 mL H_2O.

2.3. Development of marine biopolymers hydrogels

Firstly, collagens and chitosan were separately solubilized in ammonium acetate, while fucoidan was dissolved in ultra-pure water in different concentrations, 30 and 50 mg/mL for collagens, 30 mg/mL for chitosan and 100 mg/mL for fucoidan (i.e. 30 mg/mL = 3%, 50 mg/mL = 5%, and 100 mg/mL = 10%). After that, D-MEM cell culture was added to the biopolymer solution to neutralize the pH (pH verification by staining the red phenol present in the medium) in order not to compromise the viability of the cells. The solutions were then mixed following the formulations described in Table 1 using an ultra-turrax®-IKA in low rotations to form a homogenous solution (avoid bubbles) and sterilized in a Petri dish (approximately 3 mL per dish) using ultraviolet light in a laminar flow chamber for 30 min. The procedure to obtain hydrogels is shown in Fig. 1. Moreover, the molds (i.e., each of 48 plate wells) were redesigned to preserve the hydrogel structure and functionality and assess the sustainability and the 3R's policy. For this, the developed hydrogels can be removed carefully during the unmold process without damaging the structure. Furthermore, to prevent the polymer solution from escaping, a silicone film was produced and placed at the bottom of the 48-plate and fixed with an aluminum plate and screws. Likewise, each mold contains a 3D-printed cylinder produced with PLA with weights inside. The other half of the cylinder was kept empty to contain cotton inside as complementary material, helping on the absorption process together with the filters paper (digital image in Fig. 1).

Table 1
Composition of the developed hydrogels prepared by blending of 3 marine origin biopolymers solutions with the indicated concentration (between brackets is the polymer ratio in the resulting gel).

Samples	Abbreviation	Composition			
		Collagen jellyfish	Collagen shark	Chitosan squid pens	Fucoidan seaweed
Hydrogel jCOL/CHT/FUC	H_1 (100%)	5% (27.77%)	– (0%)	3% (16.67%)	10% (55.56%)
Hydrogel sCOL/CHT/FUC	H_2 (100%)	– (0%)	3% (18.75%)	3% (18.75%)	10% (62.50%)
Hydrogel jCOL/sCOL/CHT/FUC	H_3 (100%)	5% (23.81%)	3% (14.29%)	3% (14.29%)	10% (47,61%)

% of polymer in the original solution; (% of polymer in the gel formulation).

To perform a cellular encapsulation approach, each polymeric solution was mixed with a lower volume of D-MEM medium (50 μL) that contains a higher concentration of cells, being calculated 1 M cells per each mL of polymeric solution, to do not change the polymeric volume significantly, and then were distributed on the 48 CAMPH plate wells and put on the top of each well, filter paper strips to absorb the residual water. Afterward, the plate was incubated at 37 °C for approximately 30 min. The filter papers absorbed the liquid solution during the incubation time and compacted the biopolymers, producing a polyelectrolyte complex by natural cross-linking.

2.4. Physico-chemical characterization of hydrogels

2.4.1. Scanning Electron Microscopy (SEM)

The morphology of each COL/CHT/FUC hydrogel was analyzed with a Nova NanoSEM 200 scanning electron microscope (SEM) (JSM-6010LV, JEOL, Tokyo, Japan). For this analysis, the hydrogels were inserted into the desiccator for 3 days to remove the residual liquids, obtaining a dry material without using freeze-drying that would promote the formation of a porous structure. The samples were then fixed on aluminum stubs using a mutual conductive adhesive tape and covered with gold using a Leica EM ACE600 sputter coater.

2.4.2. Water uptake

The water uptake ability of developed COL/CHT/FUC hydrogels was studied, by weight variation upon incubation in aqueous solution. The dehydrated biomaterial (W_0) was immersed into Dulbecco's modified Eagle's medium-low glucose (DMEM, Sigma-Aldrich, USA) (pH = 7.4) supplemented with 10% fetal bovine serum (Alfagene, USA) and 1% antibiotic/antimycotic solution (Gibco, UK) at 37 °C during 21 days. At different time points (1, 2, 3, 6, 12 h and 1, 3, 7, 14, and 21 days), the samples were withdrawn, the excess solution was absorbed with dried filter paper, and then weighed immediately (W_w). The percentage of DMEM cell culture medium absorbed by samples was calculated with

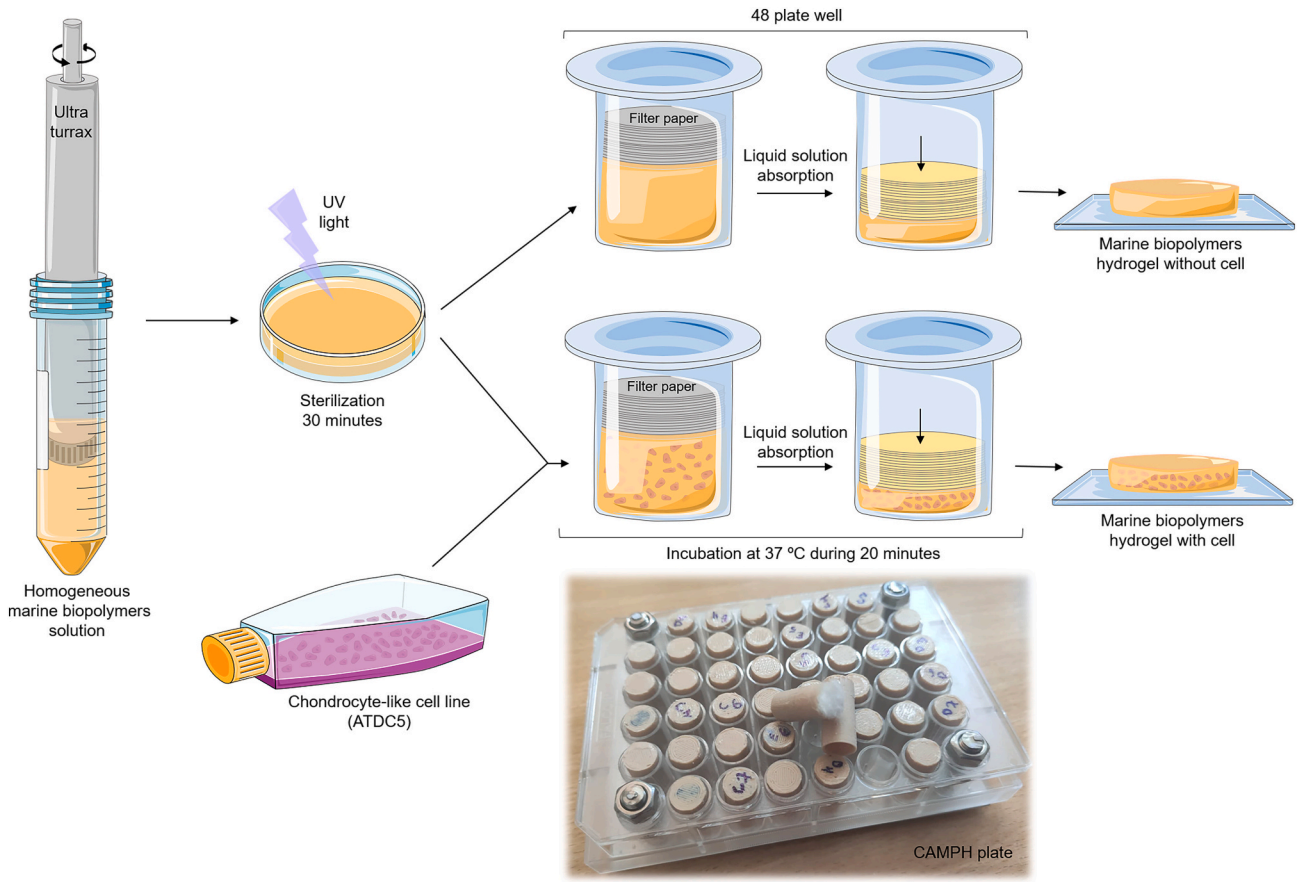

Fig. 1. Schematic representation of marine hydrogel formation process with and without cells, being demonstrated a digital image of the developed CAMPH plate.

the following Eq. (2):

$$\text{DMEM uptake } (\%) = (W_w - W_0)/W_0 * 100 \quad (2)$$

2.4.3. Degradation assays

The degradation rate of the COL/CHT/FUC hydrogels was studied according to ISO 10993-13: Biological evaluation of medical devices-Part 13: Identification and quantification of degradation products from polymers and by ISO 10993-9: Biological evaluation of medical devices-Part 9: Degradation of materials related to biological testing. The initial weight of the biomaterials was recorded as Wi, followed by immersion in 5 mL of PBS (Phosphate-Buffered Saline) containing 20 ng/mL of collagenase from *Clostridium histolyticum*, 8 mg/L of lysozyme from chicken egg white, and 2.6 U/mL of hyaluronidase from sheep testes type II, incubated at 37 °C at different time points (1, 3, 6, 12 h and 1, 3, 7, 14, 21, and 30 days). After each incubation period, the hydrogels were dried using filter paper to determine the wet weight of the samples and then frozen overnight and freeze-dried to obtain the dry weight of the samples (W_{fd} – $weight_{freeze\text{-}dried}$). The degradation rate (Eq. (3)) and the determination of water uptake during the degradation test (Eq. (4)) was calculated using the following equations, respectively:

$$\text{Degradation } (\%) = (W_i - W_f)/W_i * 100 \quad (3)$$

$$\text{Water uptake after degradation } (\%) = (W_i - W_{fd})/W_{fd} * 100 \quad (4)$$

2.4.4. Rheology assays

Rheological analyses were performed using a Kinexus pro+ rheometer (Malvern Instruments, UK), with the acquisition being accomplished using software from Malvern: rSpace. The measuring plate-plate system used in these trials was equipped with an upper measurement geometry (8 mm of diameter) and a lower plate pedestal, both in stainless steel (316 grade) with a rough finish to prevent sample slipping. Oscillatory experiments were performed to study viscoelasticity. Linear viscoelastic region (LVER) for the wet scaffolds ($d \sim 8$ mm and $h \sim 2$ mm) was determined through a strain sweep test (0.01–1%) at a constant frequency (1 Hz) and room temperature. Frequency sweep curves were afterward obtained. All plots were built by an average of at least three experiments. First, the adhesivity of materials was measured using pull away experiments in a rheometer, which involved loading a sample and then pulling away from the upper plate from the lower pedestal at a defined gap speed (1 $mm \cdot s^{-1}$), with 2 s and 1 N of contact time and contact force, respectively. Then it was recorded the normal force as a function of the gap. Finally, the area under the force-gap curve was used to determine the adhesion strength. Each experimental condition was at least repeated three times.

2.5. Marine biomaterials - biological evaluation

2.5.1. Evaluation of cell viability – MTS assay

The effect of hydrogels MEM extracts on the metabolic activity of chondrocyte-like cell line (ATDC5) was quantified with the MTS assay that evaluated the bioreduction of a tetrazolium compound, 3-(4,5-dimethylthiazol-2-yl)-5-(3-carboxymethoxypheyl)-2-(4-sulfofenyl)-2H-tetrazolium (MTS) (cell titer 96 aqueous solution cell proliferation assay, Promega, USA). Briefly, 2.5×10^4 cells/well were cultured in a 48 well plate in Dulbecco's modified Eagle's medium-low glucose (DMEM, Sigma-Aldrich, USA) supplemented with 10% fetal bovine serum (Alfagene, USA) and 1% antibiotic/antimycotic solution (Gibco, UK) for 24 h. After this time, the medium was replaced by the different hydrogel MEM extracts, for this, the leachables were obtained by incubating hydrogels in contact with the cell medium for 24 h at 37 °C. Cell culture medium was used as a negative control for cell toxicity, and latex was

used as a positive control for cell death. The bioreduction of MTS was quantified by UV-spectroscopy, reading the absorbance at 490 nm in a microplate reader (Synergy HT, Bio-Tek Instruments, USA).

2.5.2. Live/dead cell viability assay

The viability of ATDC5 cells encapsulated in the developed hydrogels was evaluated by live/dead assay using Calcein-AM (diluted 1:1200) and propidium iodide (PI) (diluted 1:300) staining. The Calcein-AM was used to label the cytoplasm of living cells by marking the esterase activity (green fluorescence). Simultaneously, PI was used to label dead cells nuclei in red fluorescence. The encapsulated cells, 1 M cells per mL of polymeric solution, were cultured in a 48 well plate using D-MEM low glucose and cultured for up to 7 days. Stained cells were imaged along the hydrogels using a Transmitted and Reflected Light Microscope with Apotome 2 (Zeiss – Axio Imager Z1m) at 5× magnification.

2.5.3. Cell morphology and cytoskeletal organization assessment (phalloidin DAPI)

The morphology of ATDC5 cells was checked by Phalloidin and DAPI staining. Phalloidin (5 μL in 1 mL of PBS) was utilized to stain the actin cytoskeleton (red fluorescence) and DAPI (4′,6-diamidino-2-phenyindole, 2 μL in 1 mL of PBS) to stain the nucleus (blue fluorescence). The encapsulated cells, 1 M cells per each mL of polymeric solution, were cultured in a 48 well plate using D-MEM low glucose, up to 7 days in different time points (1, 3, and 7 days). Stained cells were imaged using a Transmitted and Reflected Light Microscope with Apotome 2 (Zeiss – Axio Imager Z1m) at a magnification of 20×.

2.6. Statistical analysis

Statistical analysis was performed by two-way ANOVA followed by Tukey's post hoc test, using GraphPad Prism 8.0.1 (GraphPad Software, Inc., La Jolla, Ca). Differences between the groups with a confidence level of 95% ($p < 0.05$) were considered statistically significant. All results are presented as mean ± standard deviation. The significance level between the groups were represented by symbols of * ($p < 0.05$), ** ($p < 0.01$), *** ($p < 0.001$), **** ($p < 0.0001$), and by *ns* (no significance). All data were presented as mean ± standard deviation (SD).

3. Results and discussion

3.1. Characterization of the marine origin biopolymers

3.1.1. Amino acid analysis

The amino acid contents of two types of collagens from different origins (jellyfish and shark) were analyzed to determine the composition in terms of amino acids, with the results being expressed as total residue per 1000 residues in Table 2.

The studied collagens present a higher presence of glycine (293 and 334 residues), alanine (88 and 118 residues), and glutamic acid (104 and 77 residues), followed by proline, aspartic acid, and hydroxyproline. The triple-helical sequence of collagen (stable molecule) is composed essentially by repeat model $(Gly\text{-}X\text{-}Y)_n$, where X and Y typically can be proline and hydroxyproline respectively, except in the telopeptide regions [28], the first 14 and 10 amino acid sequences present in the N- and C- Terminus, respectively [29,30]. Accordingly, glycine is the major amino acid in the collagen structure, corresponding to nearly one-third of the total amino acids. Total proline (Pro) and hydroxyproline (Hyp) contents of jellyfish and shark collagen were 96 and 157 residues/1000, respectively. These contents are correlated with the species, habitat (lower or higher temperatures) and highlight the thermal stability of the collagen helix since the amino acids of Pro and Hyp are involved in the formation of junction zones stabilized by inter-chain hydrogen bonding between the carbonyl groups of the polypeptides composing the triple helix [31,32]. Thus, these contents are associated with the denaturation temperature of the collagen, for this, it is expected that the collagen from sharks may render higher denaturation temperature when compared with collagen from jellyfish [32–34]. Also, if the contents of hydroxyproline increase, the mechanical properties as measured by rheology and the gel strength are expected to increase, given the higher number of intermolecular bonds formed by this amino acid [35]. Additionally, it has been reported that type II collagens frequently had low contents of methionine, histidine, cysteine, and tyrosine, which occurs in many marine origin collagens, such as jellyfish, fish, or from shark [36,37].

Table 2
Amino acid compositions of collagen from jellyfish (jCOL) and collagen from blue shark (sCOL) (residues per 1000 total amino acids residues)

Amino acid	jCOL (mol ‰)	sCOL (mol ‰)
Aspartic acid (Asp)	84.48	43.44
Threonine (Thr)	39.34	21.93
Serine (Ser)	54.33	45.86
Glutamic acid (Glu)	104.40	77.77
Glycine (Gly)	293.11	325.46
Alanine (Ala)	88.90	118.93
Cysteine (Cys)	5.28	3.56
Valine (Val)	28.44	21.36
Methionine (Met)	8.18	17.38
Isoleucine (Ile)	17.03	15.67
Leucine (Leu)	34.23	25.64
Norleucine (Nleu)	17.20	13.82
Tyrosine (Tyr)	10.56	6.55
Phenylalanine (Phe)	21.29	18.80
Hydroxylysine (OHlys)	25.72	6.98
Histidine (His)	4.09	7.69
Lysine (Lys)	22.99	25.50
Arginine (Arg)	44.11	45.86
Hydroxyproline (Hyp)	29.82	65.56
Proline (Pro)	66.50	92.24
Total	1000	

3.1.2. Circular dichroism

The circular dichroism (CD) was used to characterize the structural compliance and the denaturation temperature of the studied collagen. Fig. 2a) demonstrates the CD spectra of the two collagens in the wavelength range of 180–240 nm. Each spectrum represents the profile obtained for collagen from jellyfish (Fig. 2**-a1**) and for collagen from shark samples (Fig. 2**-a2**). Two important peaks are observed, a positive peak at 220 nm and a negative peak at approximately 198. This kind of profile is reported in the literature for being characteristic of the presence of a triple-helical collagen structure and random coil, respectively [38–40]. However, it is noticed in Fig. 2-a1 some interferences, which may be related to some structural instability of protein to maintain the triple helix during the process of dissolving the sample in acid solution or some part of the protein has denatured, this behavior isn't noted on shark sample.

According to statistical analysis, the denaturation temperature point to be 30.8 °C ± 1.28 for the jCOL sample and 32.3 °C ± 0.34 for sCOL, determined by applying a sigmoidal curve to the variation of molar ellipticity at 220 mm with increasing temperature and calculating the inflection point. Above these reference values, the collagen is completely denatured, which is directly related to the structural loss of the triple helix, and the positive peak at 220 mm would not be visible [41]. Compared with other collagen samples in the literature, similar profiles are possibly observed [42–44]. As described above, the denaturation temperature is directly related to the Pro and Hyp contents. According to the results, if we associate the CD results and the values of hydroxyproline and proline, the sCOL presents a higher content of Pro and Hyp than jCOL, which can indicate more structural stability of the former and is in agreement with the observed highest denaturation temperature.

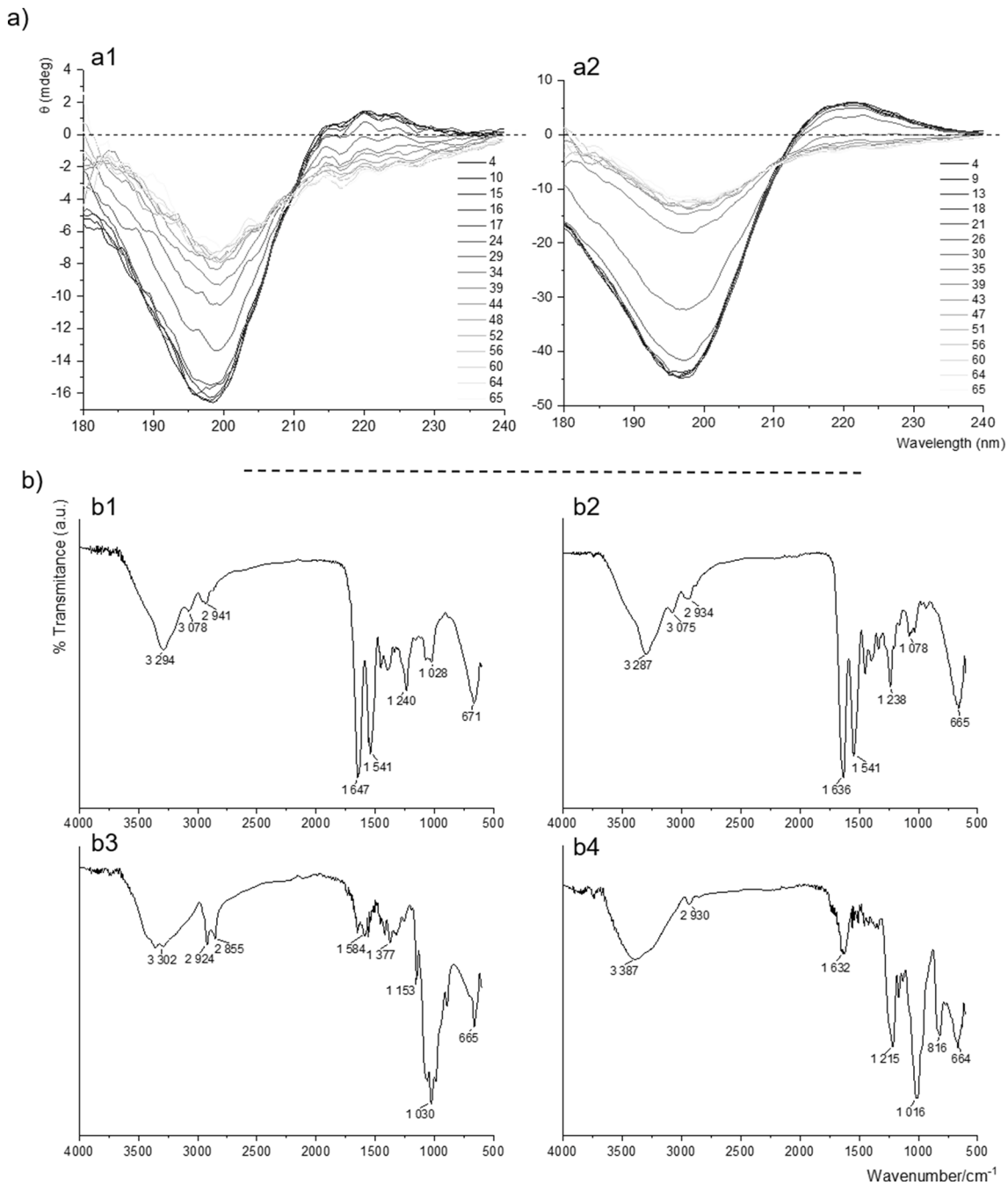

Fig. 2. Marine biopolymers spectroscopically characterization: **a)** CD spectra of the jCOL (**a1**) and sCOL (**a2**) obtained at different temperatures; **b)** Attenuated Total Reflectance – Fourier Transform InfraRed (ATR - FTIR) spectra of **b1)** collagen from jellyfish; **b2)** collagen from blue shark; **b3)** chitosan from squid pens and **b4)** fucoidan from brown algae.

3.1.3. Attenuated Total Reflectance – Fourier Transform InfraRed (ATR-FTIR) spectroscopy

The FTIR spectra of the different marine biopolymers studied in this work are shown in Fig. 2b. The spectra **b1)** (jCOL) and **b2)** (sCOL) correspond to collagen samples, which contain a typical profile of characteristic bands of the collagen. The amide A band of jCOL and sCOL was found at 3294 cm^{-1} and 3287 cm^{-1}, respectively, associated with the N—H stretching vibration and suggests the existence of hydrogen bonds, probably due to a carbonyl group of the peptide chain. [30,45]. The amide B band can be observed in the range between 3000 and 2870 cm^{-1}, which corresponds to an asymmetrical stretching of CH_2 [36]. The occurrence of the peaks at 2941 and 2934 cm^{-1} confirm the presence of amide B in these collagen samples. The amide I band arises between 1650 and 1635 cm^{-1}, with the peaks in the spectra of the studied collagen being observed at 1647 and 1636 cm^{-1}, respectively. This band corresponds to the stretching vibration of C═O (carbonyl) groups in proteins, which can be used to analyze the secondary structure [45,46]. The peak of the amide II band is observed typically near 1540 cm^{-1}, being observed in both collagen at 1541 cm^{-1}, this amide is associated with N—H bending vibration coupled with C—N stretching vibration [30,47]. In addition, the amide III bands of jCOL and sCOL were found at the wavenumber of 1240 cm^{-1} and 1238 cm^{-1}, respectively, and are associated with N—H deformation and C—N stretching vibration [48]. In general, the profile obtained for jCOL and sCOL are similar to the FTIR spectra of collagens obtained from other marine species described in the literature [49–52]. The FTIR spectrum **b3)** corresponded to the chitosan

sample (sCHT) and exhibited broadband in the range of 3600–2700 cm^{-1} with a peak at 3302 cm^{-1}, which is typically associated with the intramolecular hydrogen bonding between the stretching vibration of the N—H stretching vibration of the chitosan biomacromolecule [53,54]. The results demonstrated peaks at 1657, 1584, and 1377 cm^{-1}, assigned to amide I, amide II, and amide III bands, corresponding to vibration of C═O and N—H (amide I), vibration of N—H (amide II), C—H (amide III), while the peaks obtained between 1200 and 950 cm^{-1} are associated with C-O-C and C—O bonding. The FTIR chitosan profile is similar to the one obtained with chitosan from described in the literature [54–56].

The fucoidan from brown algae was also characterized by FTIR, with the representative characteristics peaks being shown in the spectrum in Fig. 2**-b4)**: a large band centered around 3387 cm^{-1}, attributed to the hydrogen-bonded O—H stretching vibration; a low-intensity peak at 2930 cm^{-1} for the aliphatic C—H [57]; an important peak at 1632 cm^{-1} corresponding to the asymmetric stretching of the O—C—O vibration, connected the absorbance of uronic acid [58]; the S═O stretching peak at 1215 cm^{-1} related to the presence of sulfate groups [59,60]; the band around 1016 cm^{-1} associated to glycosidic links [61,62]; the absorption peak around 816 cm^{-1} attributed to the C—O—S bending vibration of sulfate substituents [60,61] and in addition a peak at 664 attributed to the asymmetric and symmetric O=S=O deformation of sulfates [58,63].

3.1.4. Sodium Dodecyl Sulfate – Polyacrylamide Gel Electrophoresis (SDS-PAGE)

The molecular weight of the studied collagen and collagen samples of reference (type I collagen from bovine skin and type II collagen from chicken) was determined by SDS-PAGE (Fig. 3a) as this technique permits the separation of denatured protein chains according to their size. The electrophoresis analysis confirmed the presence of typical patterns of the collagen, namely, β, α1, α2, and α3 chains. According to the literature, the presence of the β chain indicates the presence of intermolecular crosslinking between the polymeric chains of two collagen molecules, and the alpha 1 (α1) and alpha 2 (α2) represents the principal domains of the collagen structure: alpha polypeptidic chains [64–66]. Additionally, the presence of alpha 3 (α3) depends on the species-specific variation in collagen composition [47]. In this order, the obtained patterns suggest for sCOL a mass values of ~250, ~120, ~115, and ~80 kDa, which represents β, α1, α2, and α3, respectively. Similarities are found in the patterns of collagen from bovine skin (β = 250, α1 = 130 and α2 = 110 kDa), which indicates that collagen from shark skin is compatible with collagen-like type I. Regarding to jCOL sample, it is possible to observe the presence of three principal and distinct chains, the β, α1, and α3. The molecular weight of each pattern is close to 260, 130, and 100 kDa, respectively. The molecular weight observed on this sample is approximately 125 kDa, which is according to the type II collagen composition since they are composed of 3 identical alpha chains, and for this reason, it is expected that the first alpha band comprises a higher intensity, approximately between 100 and 130 kDa. Similar patterns are observed in type II collagen from chicken (column 2), which have mass values near 260, 130, and 115 kDa, corresponding to β, α1, and α2 chains. These comparations suggest the studied jCOL shares similarities with collagen type II, according to the evidence previously found indicating an ancient role for jellyfish collagen, sharing features with different types of human collagens [67]. The jCOL results are consistent with the results obtained by the SDS-PAGE provided by the company Jellagen Pty Ltd. (UK), which indicates the sample is a collagen-like protein, with a high oligomer content and don't have indications of low molecular weight contaminants (not being visible also in our result). The literature reports similar patterns with collagen from analogous species to the studied samples [50,68,69].

3.1.5. X-ray diffraction (XRD)

The XRD analysis was performed to recognize some structural aspects of the studied collagen. As shown in Fig. 3b, the diffraction patterns of jCOL and sCOL coincide with other spectra found in the literature [49,70] and are composed of a peak at 12.5°, due to the presence of a triple helix. Shifts can occur on diffraction angle (2θ), related to the arrangement of the triple helix, types of collagen, and species (mammal or marine) [71,72]. According to the Bragg equation, the observed peaks correspond to a d value of 7.24 Å for the jCOL sample and 7.11 Å for sCOL, which are associated with the distance of the molecular chains of the triple helical structure. The broad peak (amorphous scatter) that appeared around 40–50 (2θ) results from unordered components of the protein [70].

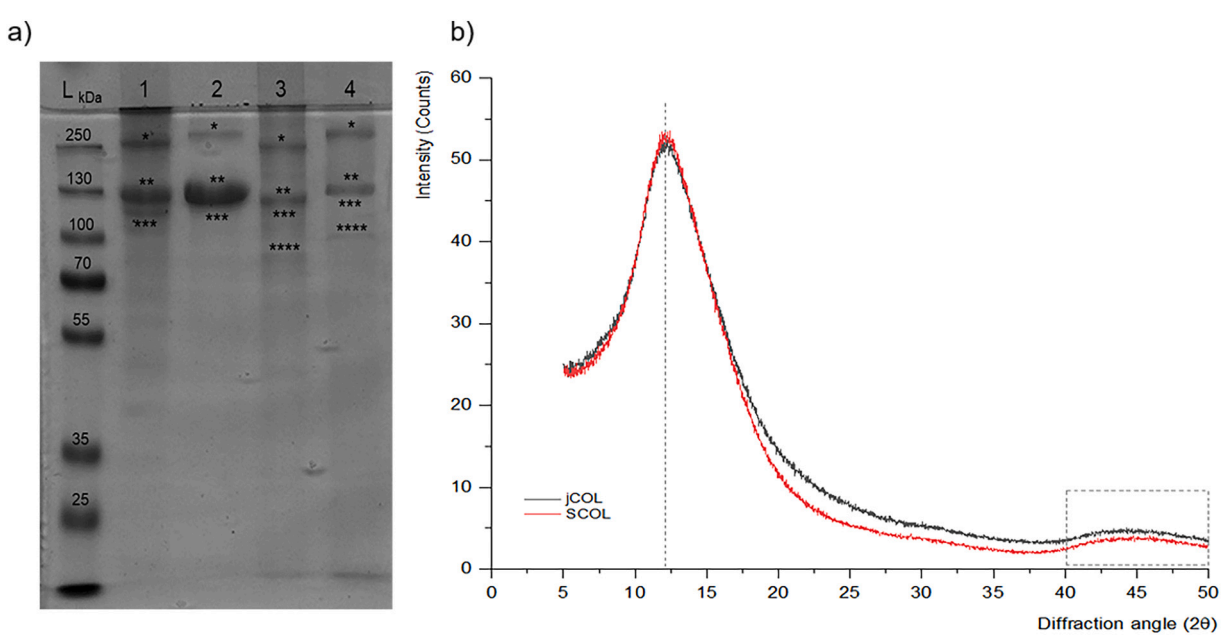

Fig. 3. Marine biopolymer characterization; **a)** SDS-PAGE (9%) pattern of analyzed collagen samples. L: Page Ruler Prestained protein ladder – 0 to 250 kDa; 1: standard collagen from bovine skin (type I); 2: standard collagen from chicken (type II); 3: collagen from shark (sCOL) and 4: collagen from jellyfish (jCOL). The symbols of *, **, *** and **** correspond a different pattern, that * indicates the β chain, ** to α_1 chain, *** to α_2 chain, and **** to α_3 chain; **b)** XRD spectra of collagen from jellyfish (jCOL) and collagen from shark (sCOL).

3.1.6. Inductively Coupled Plasma (ICP) spectrometer

Heavy metals, metals, and other elements such as Arsenic (As), Cadmium (Cd), lead (Pb), Strontium (Sr), Iron (Fe), Mercury (Hg), Calcium (Ca), and Sodium (Na) can be found in marine sources, raising concerns due to their capacity to accumulate in living tissues, being consequently potentially toxic to the organisms. Therefore, to determine the feasibility of using the studied marine biopolymers in tissue engineering and regenerative medicine as biomaterial, the content of some elements was analyzed by ICP-AES and ICP-MS. The results are shown in Table 3.

Some entities, such as U.S. Pharmacopeia Convention (USP), and U. S. Food and Drug Administration (FDA), European Medicines Agency (ICH guideline Q3D (R1) on elemental impurities), and International Organization for Standardization (ISO), have defined guidelines to specify the maximum limits for the amounts of elemental impurities in products, according to the daily dose permitted (based on a 50 kg person), as drug products, cosmetics, and food (values for Parenteral Component Limit) [73–76]. In the present study, the results demonstrated that all studied elements present in each marine sample, highlighting the elements Al, Ag, Au, Ca, Cu, Fe, K, Mg, Mn, Na, P, Sr, and Zn, are present in low amounts and below the listed limits. However, some heavy metals such as As, Cd, Hg, or Pb were detected in some samples in quantities slightly above the tabulated reference values, which can compromise the cells viability and promote some mortality.

Unfortunately, these guidelines aren't specific for biomaterials envisaging the use in biomedical applications, and there is still a need to create new regulations for the limits of heavy metal and metal impurities in natural samples considering the specific application and potential body uptake.

3.2. Production of marine biopolymers hydrogels and physical-chemical characterization

The present work introduces a recent innovative methodology for preparing polymeric systems compliant with cell encapsulation, as described in the experimental section (2.3). The efficiency of the proposed eco-friendly method to produce both cell-free and cell-laden hydrogels was first assessed by observing the cohesiveness of the systems and their handleability, namely using forceps, with all formulations withstanding manipulation, including when incubated in an aqueous solution or cell culture medium.

Table 3
Elementary contents present on studied marine source. **jCOL** – collagen from jellyfish; **sCOL** – collagen from shark; **sCHT** – chitosan from squid pens; **aFUC** – fucoidan from brown algae.

Elements	Content of each sample (ppm)				National standard (ppm)
	jCOL	sCOL	sCHT	aFUC	
Al	<10	195	<10	173	500
As	<4	<4	<4	<4	1.5
Ag	<0.2	30	0.5	<0.2	50
Cd	<0.1	<0.1	<0.1	0.9	0.5
Hg	<0.1	1.5	<0.1	<0.1	0.5
Pb	<0.2	3.9	<0.2	0.8	0.5
Au	<0.1	<0.1	<0.1	<0.1	1
Cu	0.4	0.3	0.3	<0.6	10
Fe	0.3	0.3	0.3	0.5	150
Zn	<0.1	<0.1	<0.1	<0.1	150
Mg	<1	<0.4	<0.4	<10	Under deliberation
Mn	<0.3	<0.3	<0.4	<0.4	70
Sr	0.5	0.5	0.5	<2	300
Ca	1	1	<0.4	19.8	–
K	0.5	0.5	0.5	31.5	–
Na	3.3	0.4	<0.5	<10	–
P	1.5	3.0	<0.1	<0.2	–

3.2.1. Morphology by Scanning Electron Microscopy (SEM)

The surface morphology of the developed hydrogels was investigated by scanning electron microscopy. In Fig. 4a, it is clearly noticed that all hydrogel systems presented a compact structure promoted by the CAMPH methodology, being observed the occasional appearance of few pores, but not uniformly distributed in the structure. Nevertheless, by comparing the images illustrating the different formulations, it seems that the presence of jellyfish collagen resulted in a less porous structure, eventually due to a stronger interaction and aggregation of the enrolled biopolymers.

3.2.2. Water uptake abilities

The water uptake test was performed to appreciate the swelling ability of the developed hydrogels, as shown in Fig. 4b. The results demonstrated that all formulations have the ability to reabsorb liquids (DMEM cell culture medium) after being dehydrated. Moreover, they were capable of absorbing large quantities of culture medium in the first 24 h, after this, the hydrogels tend to maintain the weight (saturation phase) approximately during 20 days until some natural degradation of the polymers or hydrogel disassembly starts to be visible. During the experimental time, it is clearly verifiable that all profiles exhibited a great capacity to absorb liquids, with H_2 and H_3 showing more stability and less natural degradation when compared with H_1, which can be useful when the envisaged biomedical approach needs a longer exposure time. It is also visible by the naked eye the natural degradation of H_1 on the last time point (Fig. 4c-4) after 21 days of incubation when compared with the previous timepoint (Fig. 4c-3; temporal difference of 168 h). Furthermore, during the experiment, it was verified that the developed hydrogels are compliant with physiological temperature (37 °C) without compromising their structure.

3.2.3. Degradation rate assay

The physiological polymer degradation is an important key for tissue engineering to understand the biomaterials degradation time-scale. It is vital to coincide with the regeneration/healing process time-scale to ensure the proper remodeling of the targeted tissue [77]. Actually, several factors influence the degradation rate of the polymers, such as thermal-, mechanically, type of chemical bond, pH, (co)polymer composition, water uptake, chemically and enzymic [78,79]. In this work, we addressed the hydrogel degradation by enzymatic reaction using collagenase, hyaluronidase, and lysozyme with a similar concentration to the one found in human blood plasma [80,81] results being depicted in Fig. 5**a**, **b**, and **c)**. Collagenase is an enzyme that can be found in all multicellular animals, responsible for breaking the peptides bonds and cleaving the triple-helical structure of collagen [82]. Hyaluronidase can be found in the human body, and it is responsible for cleaving the hyaluronic acids (HA), acting on (1-4)-linkages between the *N*-acetylglucosamine and glucuronate [83]. Additionally, it is reported in the literature that this enzyme can also act on the catabolism of chondroitin sulfates (CS), although with slower action than in HA [84]. Although our formulations do not contain hyaluronic acids nor chondroitin sulfates, marine biopolymers with similar glycosidic bonds were used, as chitosan and fucoidan. Chitosan is a polysaccharide composed of D-glucosamine and *N*-acetyl-D-glucosamine, being structurally identical with monomers of HA and can be degraded by hyaluronidases and/or lysozymes [85], namely considering that the human body doesn't contain chitosanases (an enzyme responsible for cleaving chitosan). Lysozymes is a glycoside hydrolase that acts on 1,4-beta-linkages between acetylmuramic acid and *N*-acetyl-D-glucosamine residues in peptidoglycan [86].

On the other hand, fucoidan is a sulfated polysaccharide not available also in the human body (neither its specific enzyme, fucoidanase) but sharing a structural composition with sulfated glycosaminoglycans (GAG's), namely chondroitin sulfates [87]. Unfortunately, fucoidan cannot be hydrolyzed by lysozyme since it contains α(1-3) glycosidic linkages in its structure instead of (1-4) glycosidic linkages [88].

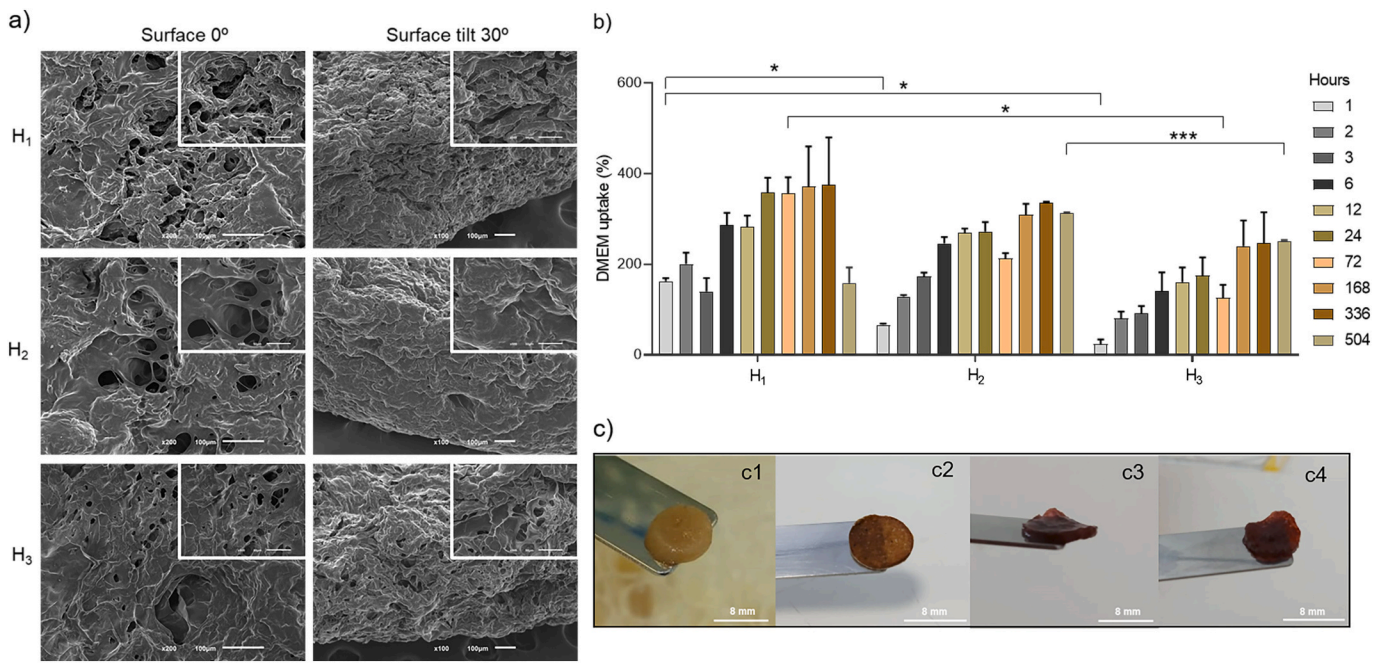

Fig. 4. Marine hydrogel characterization: **a)** Scanning Electron Microscope (SEM) images of the developed hydrogels H_1 – jCOL/CHT/FUC; H_2 – sCOL/CHT/FUC; and H_3 – jCOL/sCOL/CHT/FUC). The images in surface 0° were obtained at the magnification of 200× (scale bar: 100 μm) and 500× (scale bar: 50 μm), and images in surface tilt 30° were obtained at the magnification of 100× (scale bar: 100 μm) and 500× (scale bar: 50 μm). **b)** Assessment of the degree of swelling in each hydrogel (H_1, H_2, and H_3), immersing in DMEM cell culture medium for 21 days (504 h). Data are mean ± standard error ($n = 3$, statistical significance for * $p < 0.05$ and *** $p < 0.001$). **c)** Digital photographs of one condition hydrogel (H_1) (representative of all hydrogel studies) during the water uptake time, which **c1)** hydrogel as prepared, **c2)** dehydrated hydrogel, **c3)** hydrogel after 14 days (336 h), and **c4)** after 21 days of incubation in DMEM cell culture medium.

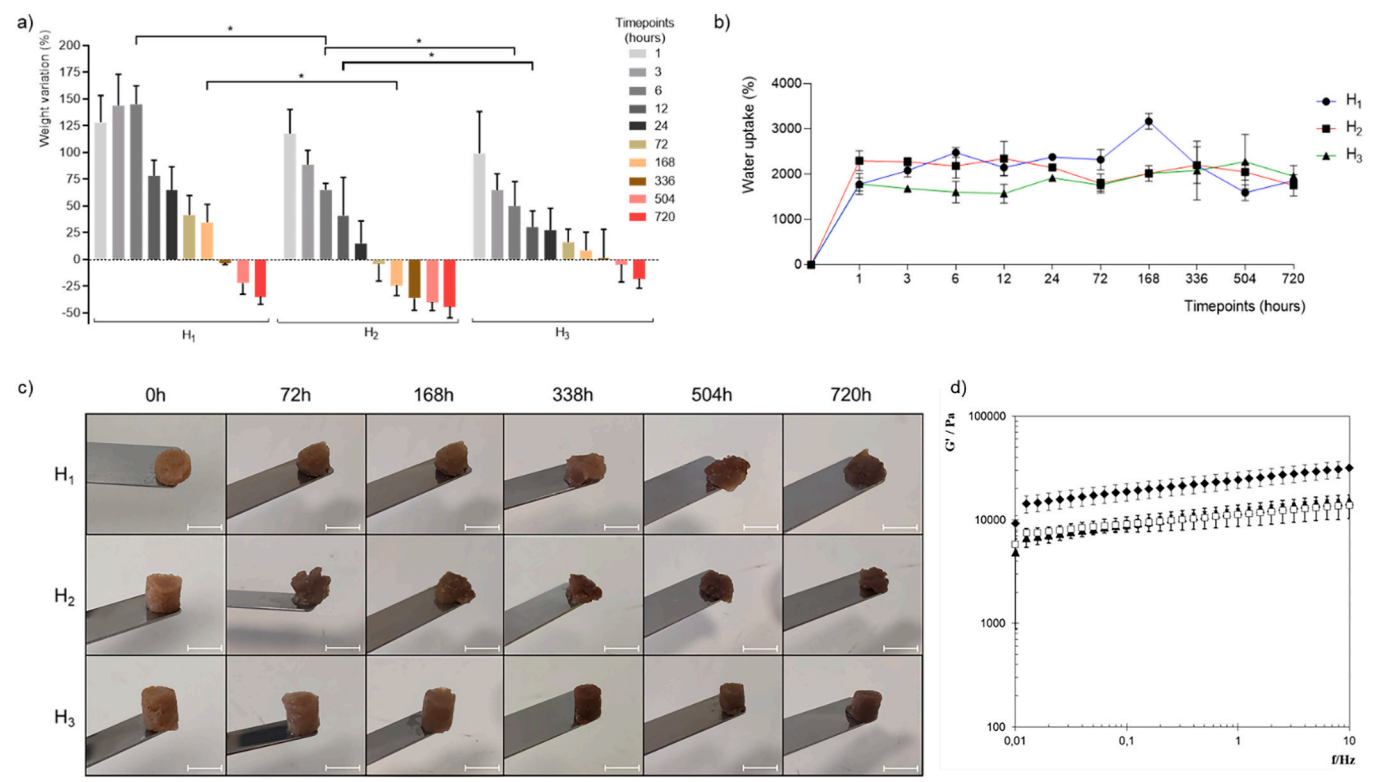

Fig. 5. Marine hydrogel characterization (enzyme degradation): **a)** assessment of weight variation as a measure of hydrogel degradation using an enzyme cocktail solution (collagenase, hyaluronidase, and lysozyme in PBS), during 30 days at 37 °C. **b)** Assessment of water uptake contents during the degradation time. **c)** Digital photographs of the three hydrogel formulations during the experiment time, showing the most relevant timepoints (0, 72, 168, 338, 505, 720 h), scale bar of 6 mm. **d)** Oscillatory rheological behavior of different marine hydrogels that were showing the elastic modulus (G′) as a function of the frequency. Values are mean ± SD of three independent experiments, (◆) H_1 – jCOL/CHT/FUC; (▲) H_2 – sCOL/CHT/FUC; and (□) H_3 – jCOL/sCOL/CHT/FUC.

Additionally, human body doesn't have enzymatic capacity to promote the degradation of fucoidan but it is known that some fucoidan samples can inhibit the action of hyaluronidase [89], from which we used the lysozyme to act on chitosan in case of the hyaluronidase stay inactive.

In the present research, all these actions can be related to the ability of the hydrogels to last several days (more than 30 days). In Fig. 5a it is demonstrated the weight variation for all conditions when submitted to the enzymatic cocktail solution. Initially, all hydrogels formulations had the ability to absorb water, and after a few days, they have lost weight and further disassembled, losing polymer mass. The formulation that could resist more time until start the degradation was the H_3 (between day 14 and 21), presenting around 18% mass loss over the 30 days, while H_1 and H_2 have a loss of mass around 35% and 44%, as can be appreciated in Fig. 5c. The water uptake ability of the hydrogels during the degradation test was also assessed (Fig. 5b). The results have shown, for all formulations, that the water uptake occurred quickly within 1 h (increased for around 2000%) and maintained roughly constant during the entire experiment. Additionally, it is important to highlight the geometry of the hydrogels, being visible in Fig. 5c that the H_3 was the formulation that could keep its initial geometry for a longer time when compared to the other formulations (H_1 & H_2). Also, the size of the hydrogels (all biomaterials were made on 96 plate wells, with the same volume of solutions) can be related to the collagen used since chitosan and fucoidan amounts used were the same in all formulations. The formulation that contains shark collagen (H_2) is bigger than the formulation with jellyfish collagen (H_1), despite having less amount of protein, showing the impact of the differences of the two collagens used on polymers assembly: when we mixed both collagens together (H_3) the size of the hydrogel is the biggest, as more polymers are present.

3.2.4. Rheology assay

The rheology of different marine hydrogels was performed to appreciate their mechanical properties, basically the resistance to shear stress as a mimic of the natural force applied by the locomotion and wear after implantation in articular cartilage as a therapeutic biomaterial. For this purpose, to assess the appropriate strain and frequency range for linear viscoelastic behavior, G' (or elasticity modulus), G'' (or viscosity modulus), and G''/G' (or loss tangent, tan δ) were determined as a function of shear frequency (Fig. 5d).

In general, the results for all hydrogels were very similar between them, especially H_2 (sCOL/CHT/FUC) and H_3 (jCOL/sCOL/CHT/FUC), with G' values increasing from 4.7 kPa to 13.8 kPa throughout the frequency sweep performed. Despite their similarities, the H_1 (jCOL/CHT/FUC) seemed to present higher values of G' (from approximately 9.3 to 32.0 kPa), although not statistically different from the other hydrogel formulations (two-way ANOVA, **** $p < 0.0001$). Characteristically, when $G' > G''$, and tan $\delta < 1$, the behavior of samples tends to be more like a gel elastic solid character (strong gel), usually reflecting the formation/connectivity of the polymeric network [90,91]. In all developed formulations, the phase angle ($\delta/^\circ$) is close to 0° thus, tan δ is also close to 0, from which $G'' \ll G'$, indicating a mechanically stable structure by their strong elastic-solid character. Regarding these mechanical characteristics, the produced hydrogels show high potential to be applied to support the biological forces during and after implantation in articular cartilage, envisaging their use as tissue regeneration biomaterial [92]. This approach will be proved in future studies using animal models. In the literature, equivalent behavior is found using different and similar polymers composing scaffolds for biomedical approaches [93,94].

The tackiness or adhesive strength of the hydrogels plays an interesting factor, assessing their capacity to adhere to a specific place, essentially to the host lesion site upon removal of the damaged tissues, to restore them. In some cases, as in articular cartilage zones, the tissues are subjected to constant movements exerted by the day-to-day tasks; hence, the implanted biomaterials need to be pressure-resistant and able to fix to the connective tissue to avoid implant dislocations during or after surgery [95]. The adhesivity strength of each of the marine biopolymers used to develop hydrogels and of these hydrogels is shown in Table 4.

The adhesive force of each biopolymer was measured to understand their own contribution to the adhesivity, being noticed a more considerable value for fucoidan (aFUC). This behavior is in accordance with the observations by Citkowska et al. [96], which demonstrate the ratio between mucoadhesive versus contents, in which a stronger mucoadhesive property corresponds to a higher percentage of fucoidan in solution. Regarding the collagen samples, both dissolved at 5% in acetic acid (50 mg/mL), it is noticed that the adhesivity results depend on their physico-chemical properties, such as viscosity, type of collagen, and species, since for this experiment, both collagen are at same solution concentration [97].

Considering the adhesivity properties of the developed hydrogels, the results are coherent with the biopolymers since the combination of polymers increases the adhesive properties. Moreover, H_2 has a value higher than the one determined for H_1, in agreement with the collagen used to prepare the respective hydrogels (adhesivity of sCOL > jCOL), despite the differences in collagen concentration. Nevertheless, the formulation that demonstrated a better adhesivity is H_3, which indicates a particularly synergic effect of combining the two collagens with the polysaccharides.

3.3. Marine biopolymers hydrogels as templates for the culture of chondrocytes

3.3.1. Evaluation of cell viability – MTS assay

The cell viability on the produced hydrogels and their eventual cytotoxicity were assessed by evaluation of the metabolic activity of chondrocyte-like cell lines (ATDC5), as determined by MTS assay using hydrogels extracts (according to International Standard ISO/EN 10993-5 [98]), which consists of contact DMEM cell culture medium with these hydrogels. The data are shown in the graph in Fig. 5a. The results demonstrated that the extracts obtained from the marine hydrogels did not compromise the metabolic activity of cells since the percentage of activity did not significantly change when compared with negative control (cells in culture medium) (data not shown). As mentioned in ISO 10993-5, the cell viability on the extract should be ≥70% of the control group for the material to be considered non-cytotoxic. Since the percentage of viable cells exposed to the extracts remained close to 100%, these hydrogels can be considered non-cytotoxic. Previously, similar results have been observed by other authors that prove that these biopolymers aren't considered cytotoxic for cells [13,18,99].

3.3.2. Live/dead cell viability assay – calcein/PI staining

The viability of the encapsulated cells (ATDC5) on different marine collagen (jellyfish and/or shark)-chitosan-fucoidan hydrogels was assessed by fluorescence microscopy after staining with Calcein-PI. The Calcein-AM is responsible for staining the living cells, giving them a

Table 4
Adhesivity of different marine biopolymers: **jCOL** – collagen from jellyfish; **sCOL** – collagen from shark; **sCHT** – chitosan from squid pens; **aFUC** – fucoidan from brown algae; and of the different hydrogel formulations (mixture of these biopolymers): $\mathbf{H_1}$ – jCOL/CHT/FUC; $\mathbf{H_2}$ – sCOL/CHT/FUC; and $\mathbf{H_3}$ – jCOL/sCOL/CHT/FUC.

Samples	Adhesivity (N.s.)
jCOL	0.098 ± 0.003
sCOL	0.132 ± 0.014
sCHT	0.056 ± 0.002
aFUC	0.287 ± 0.021
H_1	0. 319 ± 0.038
H_2	0.343 ± 0.003
H_3	0.779 ± 0.072

green fluorescence color, and the propidium iodide (PI) stained the dead cells with a red fluorescence color. The chondrocyte cells were encapsulated onto the hydrogels and cultured for 7 days (Fig. 6b). All images demonstrate a high predominant of green fluorescence, which indicates the presence of live cells, apparently increasing with culture time. During the experiment, a continuous proliferation of cells was observed on the developed hydrogels, being visible the cell distribution on the top of the hydrogels, and also inside of the structure, which supports their capacity to sustain the cell viability when encapsulated. Recently, similar results can be found in the literature for biomaterials composed of one marine polymer [100,101] or blending two polymers [102].

3.3.3. Cell morphology and cytoskeletal organization assessment - phalloidin/DAPI staining

The ATDC5 cell morphology was observed by fluorescence microscopy after staining with Phalloidin/DAPI. The Phalloidin is responsible for staining the cytoskeleton of cells, giving the idea of the cell morphology by the presence of red fluorescence color, and the DAPI will only stain the viable cell nuclei in blue fluorescence color [103]. The results observed in Fig. 6c) indicated that the cells can completely adhere to the developed hydrogels. After 3 days of culturing (encapsulation method), the acquirement of cell stretches is visible, which indicates cell adhesion on the structure. During the experiment time (7 days), the cells continually exhibit their morphology elongated, suggesting that biomaterials have a suitable microenvironment to support the viability of cells. These results are in accordance with the Live/dead assay since it is noticed that cell growth through time is related to cell proliferation.

4. Conclusion

The CAMPH (compressive and absorption methodology of the production of hydrogels) method was established to develop polymeric biomaterials – herein demonstrated with the combination of collagen from jellyfish and shark skin, chitosan, and fucoidan – enabling both acellular and encapsulated cell approaches. In brief, this methodology promotes a compressive force on the polymeric solutions while the absorption of the residual solvents occurs, which induces their natural crosslinking based on electrostatic interactions between oppositely charged polymers with no intervention of external chemical crosslinking agents. This eco-friendly procedure rendered cohesive hydrogels in which the collagen type (from jellyfish or shark skin) affected the physico-chemical properties and biological performance. The polymeric characterization demonstrates that the collagens used have a denaturation temperature of around 30–32 °C and a molecular weight of 120–125 kDa. In contrast, concerning biomaterial characterization (such as in degradation test), the results showed a mass loss around 18% for H_3 (over the 30 days) while the H_1 and H_2, present a mass loss around 35% and 44%, respectively. Thus, in general, the results suggest that all the developed marine hydrogels are promising as template devices for

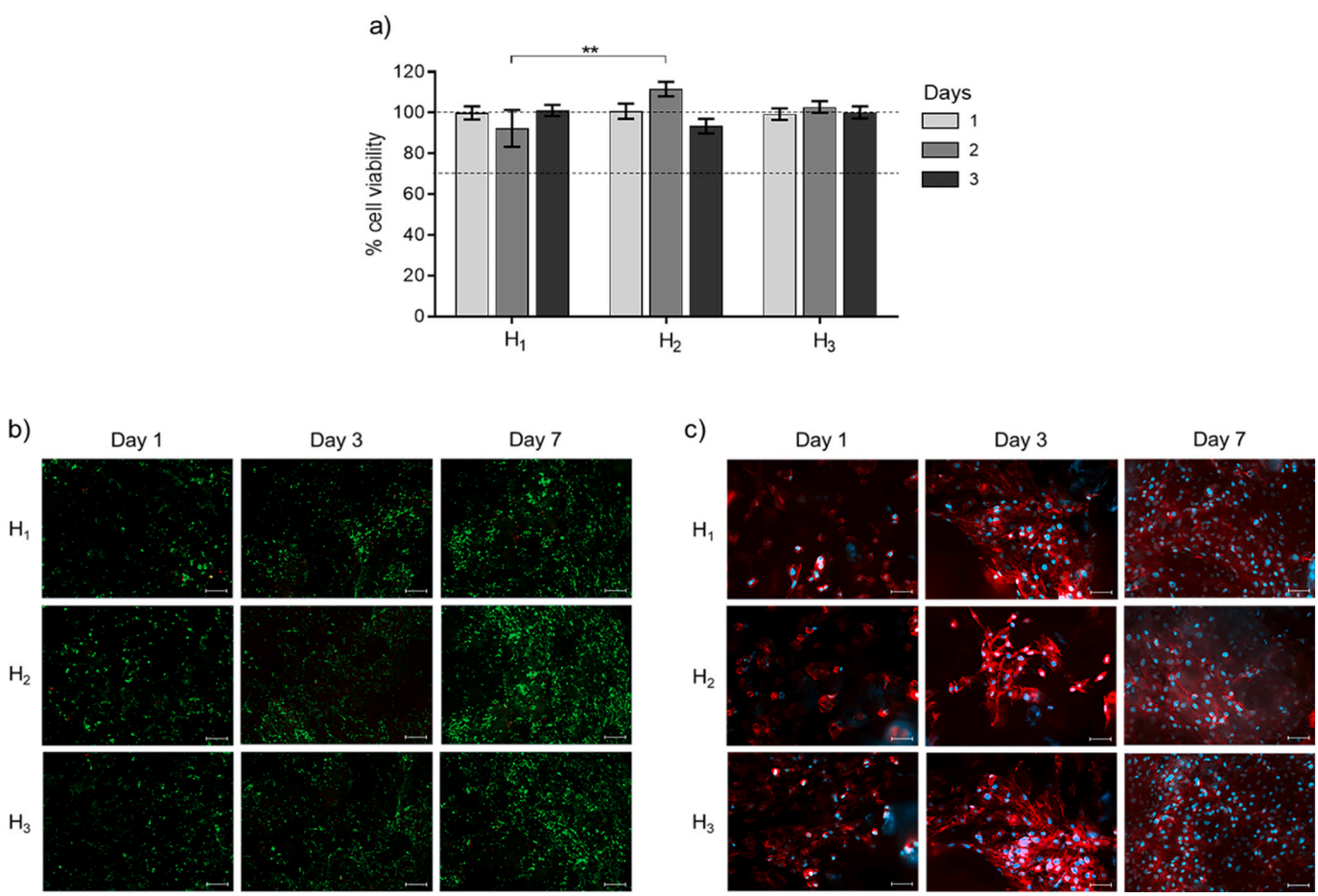

Fig. 6. In vitro biological assessment of collagen (jellyfish/shark)/chitosan/fucoidan hydrogels with a culture of ATDC5 chondrocyte cells. **a)** The cell viability percentage was determined by cytotoxicity assessment using MTS assay in different hydrogel leachables (**H_1** – jCOL/CHT/FUC; **H_2** – sCOL/CHT/FUC; and **H_3** – jCOL/sCOL/CHT/FUC). Data are mean ± standard error ($n = 3$, statistical significance for ** $p < 0.01$). **b)** Microscopy of Live/dead assay of hydrogels (H_1, H_2, and H_3), cultured up to 7 days at the magnification of 5× (scale bar 200 μm). The live cells are demonstrated in green fluorescence and the dead cells in red. **c)** Microscopy images of hydrogels (H_1, H_2, and H_3) cultured up to 7 days staining with Phalloidin DAPI at the magnification of 20× (scale bar 50 μm). The nuclei of the cells are demonstrated in blue fluorescence and the cytoskeleton in red fluorescence.

tridimensional cell culture since all supported the proliferation of chondrocyte-like cells, highlighting the formulation H_3 (jCOL, sCOL, sCHT, and aFUC) that combines both collagens as resulting in a more biomechanically stable hydrogel, interesting for future application in cartilage tissue engineering and regenerative medicine. In the future approach, the biological behavior of the hydrogels should be tested with primary chondrocyte cells (verify if maintaining their phenotype) and increase the culture time to analyze the occurrence of ECM production.

CRediT authorship contribution statement

Regarding CRediT taxonomy, the author contributions were: Carvalho, D. N.: Conceptualization; Date curation; Formal Analysis; Investigation; Methodology; Software; Visualization and writing – original draft, review & editing. Williams, D. S.; Sotelo, C. G.; Pérez-Martín, R. I. and Mearns-Spragg, A.: Resources; Validation. Reis, R. L.: Supervision; Resources; Funding acquisition. Silva, T. H.: Conceptualization; Supervision; Validation; Resources; Writing review and editing; Funding acquisition.

Declaration of competing interest

Williams, D.S. and Mearns-Spragg, A. are employees of Jellagen Ltd., the producer of jellyfish collagen used in this research. The authors report no other declaration of interest.

Acknowledgments

Carvalho, D. N., thank the Portuguese Foundation for Science and Technology (FCT) for the doctoral scholarship under the scope of doctoral program Tissue Engineering, Regenerative Medicine and Stem Cells, ref. PD/BD/143044/2018. Financial support by ERDF under the scope of Program INTERREG España-Portugal 2014–2020 through project 0245_IBEROS_1_E and under the scope of Atlantic Area Program through project EAPA_151/2016 (BLUEHUMAN) is gratefully acknowledged. The authors also thank to Jellagen Pty Ltd. (UK) for the kind offer of the collagen from jellyfish.

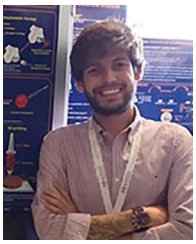

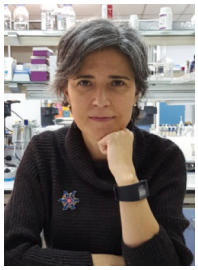

References

[1] B. Hoyer, A. Bernhardt, A. Lode, S. Heinemann, J. Sewing, M. Klinger, H. Notbohm, M. Gelinsky, Acta Biomater. 10 (2014) 883–892.
[2] X. Wu, L. Cai, A. Cao, Y. Wang, T. Li, J. Li, J. Sci. Food Agric. 96 (2016) 815–821.
[3] P. Berillis, Research trends in biochemistry, Mol. Biol. Microbiol. (2015) 1–13.
[4] L. Zhang, J. Hu, K.A. Athanasiou, Crit. Rev. Biomed. Eng. 37 (2009) 1–57.
[5] A.H. Gomoll, T. Minas, Wound Repair Regen. 22 (Suppl. 1) (2014) 30–38.
[6] C.S. Ko, J.P. Huang, C.W. Huang, I.M. Chu, J. Biosci. Bioeng. 107 (2009) 177–182.
[7] A.J.Sophia Fox, A. Bedi, S.A. Rodeo, Sports Health 1 (2009) 461–468.
[8] J.S. Temeno, A.G. Mikos, Biomaterials 21 (2000) 431–440.
[9] E. Song, S. Yeon Kim, T. Chun, H.J. Byun, Y.M. Lee, Biomaterials 27 (2006) 2951–2961.
[10] E.E. Antoine, P.P. Vlachos, M.N. Rylander, Tissue Eng. B Rev. 20 (2014) 683–696.
[11] C. Somaiah, A. Kumar, D. Mawrie, A. Sharma, S.D. Patil, J. Bhattacharyya, R. Swaminathan, B.G. Jaganathan, PLoS One 10 (2015) 1–15.
[12] C. Correia, L.S. MoreiraTeixeira, L. Moroni, R.L. Reis, C. van Blitterswijk, M. Karperien, J. Mano, Tissue Eng. Part C Methods (2011) 1–37.
[13] L.L. Reys, S.S. Silva, J.M. Oliveira, S.G. Caridade, J.F. Mano, T.H. Silva, R.L. Reis, Biomed. Mater. 8 (2013) 1–11.

[14] A. Martins, M.A. Silva, A.Costa Pinto, R.L. Reis, N.M. Neves, Bio-Inspired integration of natural materials, in: A.B. Brennan, C.M. Kirschner (Eds.), Bio-inspired Materials for Biomedical Engineering, John Wiley & Sons, 2014, pp. 125–150.
[15] A. Carretero, D. Soares da Costa, R.L. Reis, I. Pashkuleva, J. Mater. Chem. B 5 (2017) 3103–3106.
[16] T.H. Silva, A. Alves, E.G. Popa, L.L. Reys, M.E. Gomes, R.A. Sousa, S.S. Silva, J. F. Mano, R.L. Reis, Biomatter 2 (2012) 278–289.
[17] H.R. Fletcher, P. Biller, A.B. Ross, J.M.M. Adams, Algal Res. 22 (2017) 79–86.
[18] L.L. Reys, S.S. Silva, D.Soares da Costa, N.M. Oliveira, J.F. Mano, R.L. Reis, T. H. Silva, ACS Biomater. Sci. Eng. 2 (2016) 1151–1161.
[19] D.N. Carvalho, R. Reis, T.H. Silva, Biomater. Sci. 9 (2021) 6718–6736.
[20] J.T. Oliveira, R.L. Reis, Hydrogels from polysaccharide-based materials: fundamentals and applications in regenerative medicine, in: R.L. Reis, N. M. Neves, J.F. Mano, M.E. Gomes, A.P. Marques, H.S. Azevedo (Eds.), Natural-based Polymers for Biomedical Applications, 2008, pp. 485–514..
[21] V. Irawan, T.C. Sung, A. Higuchi, T. Ikoma, J. Tissue Eng. Regen. Med. 15 (2018) 673–697.
[22] D.N. Carvalho, C. Gonçalves, J.M. Oliveira, D.S. Williams, A. Mearns-Spragg, R. L. Reis, T.H. Silva, Green Chem. 23 (2021) 7016–7029.
[23] J.E. Gough, C.A. Scotchford, S. Downes, J. Biomed. Mater. Res. 61 (2002) 121–130.
[24] A.R.C. Duarte, V.E. Santo, A. Alves, S.S. Silva, J. Moreira-Silva, T.H. Silva, A. P. Marques, R.A. Sousa, M.E. Gomes, J.F. Mano, R.L. Reis, J. Supercrit. Fluids 79 (2013) 177–185.
[25] R.A. Sheldon, J. Chem. Technol. Biotechnol. 68 (1997) 381–388.
[26] G.S. Diogo, E.L. Senra, R.P. Pirraco, R.F. Canadas, E.M. Fernandes, J. Serra, R. I. Perez-Martin, C.G. Sotelo, A.P. Marques, P. Gonzalez, J. Moreira-Silva, T. H. Silva, R.L. Reis, Mar. Drugs 16 (2018) 1–14.
[27] D.N. Carvalho, R. Lopez-Cebral, R.O. Sousa, A.L. Alves, L.L. Reys, S.S. Silva, J. M. Oliveira, R.L. Reis, T.H. Silva, Biomed. Mater. (2020) 1–22.
[28] J.C. Horng, F.W. Kotch, R.T. Raines, Protein Sci. 16 (2007) 208–215.
[29] P. Kittiphattanabawon, S. Benjakul, W. Visessanguan, H. Kishimura, F. Shahidi, Food Chem. 119 (2010) 1519–1526.
[30] S. Iswariya, P. Velswamy, T.S. Uma, J. Polym. Environ. 26 (2017) 2086–2095.
[31] S. Addad, J.Y. Exposito, C. Faye, S. Ricard-Blum, C. Lethias, Mar. Drugs 9 (2011) 967–983.
[32] C.G. Sotelo, M.B. Comesaña, P.R. Ariza, R.I. Pérez-Martín, J. Aquat. Food Prod. Technol. 25 (2015) 388–399.
[33] C.L. Jenkins, L.E. Bretscher, I.A. Guzei, R.T. Raines, J. Am. Chem. Soc. 125 (2003) 6422–6427.
[34] L. Sun, B. Li, W. Song, L. Si, H. Hou, Process Biochem. 63 (2017) 229–235.
[35] J.-W. Woo, S.-J. Yu, S.-M. Cho, Y.-B. Lee, S.-B. Kim, Food Hydrocoll. 22 (2008) 879–887.
[36] E. Jeevithan, B. Bao, Y. Bu, Y. Zhou, Q. Zhao, W. Wu, Mar. Drugs 12 (2014) 3852–3873.
[37] B. Inwoo, O. Kiyoshi, Y. Asami, O. Kazufumi, Y. Atsuko, H. Kenji, Food Chem. 108 (2008) 49–54.
[38] A. Miki, S. Inaba, T. Baba, K. Kihira, H. Fukada, M. Oda, Biosci. Biotechnol. Biochem. 79 (2015) 1603–1607.
[39] X.R. Shen, X.L. Chen, H.X. Xie, Y. He, W. Chen, Q. Luo, W.H. Yuan, X. Tang, D. Y. Hou, D.W. Jiang, Q.R. Wang, Mil. Med. Res. 4 (2017) 33–45.
[40] A. Wood, M. Ogawa, R.J. Portier, M. Schexnayder, M. Shirley, J.N. Losso, Comp. Biochem. Physiol. B Biochem. Mol. Biol. 151 (2008) 246–249.
[41] K.E. Drzewiecki, D.R. Grisham, A.S. Parmar, V. Nanda, D.I. Shreiber, Biophys. J. 111 (2016) 2377–2386.
[42] A. Gopinath, S.M. Reddy, B. Madhan, G. Shanmguam, J.R. Rao, Eur. Biophys. J. 43 (2014) 643–652.
[43] J.C. Silva, A.A. Barros, I.M. Aroso, D. Fassini, T.H. Silva, R.L. Reis, A.R.C. Duarte, Ind. Eng. Chem. Res. 55 (2016) 6922–6930.
[44] L.A. Tziveleka, E. Ioannou, D. Tsiourvas, P. Berillis, E. Foufa, V. Roussis, Mar. Drugs 15 (2017) 1–17.
[45] B.B. Doyle, E.G. Bendit, E.R. Blout, Biopolymers 14 (1975) 937–957.
[46] A. Veeruraj, M. Arumugam, T. Ajithkumar, T. Balasubramanian, J. Mater. Sci. Mater. Med. 23 (2012) 1729–1738.
[47] Z. Barzideh, A.A. Latiff, C.-Y. Gan, S. Benjakul, A.A. Karim, Int. J. Food Sci. Technol. 49 (2014) 1490–1499.
[48] S. Tamilmozhi, A. Veeruraj, M. Arumugam, Food Res. Int. 54 (2013) 1499–1505.
[49] R.O. Sousa, A.L. Alves, D.N. Carvalho, E. Martins, C. Oliveira, T.H. Silva, R. L. Reis, J. Biomater. Sci. Polym. Ed. 31 (2019) 1–18.
[50] F.F. Felician, R.H. Yu, M.Z. Li, C.J. Li, H.Q. Chen, Y. Jiang, T. Tang, W.Y. Qi, H. M. Xu, Chin. J. Traumatol. 22 (2019) 12–20.
[51] W.K. Song, D. Liu, L.L. Sun, B.F. Li, H. Hou, Mar. Drugs 17 (2019) 1–14.
[52] J. Elango, Y. Bu, B. Bin, J. Geevaretnam, J.S. Robinson, W. Wu, Food Biosci. 17 (2017) 42–51.
[53] H. Staroszczyk, K. Sztuka, J. Wolska, A. Wojtasz-Pajak, I. Kolodziejska, Spectrochim. Acta A Mol. Biomol. Spectrosc. 117 (2014) 707–712.
[54] A. Shavandi, A.E.-D.A. Bekhit, Z. Sun, M.A. Ali, J. Sol-Gel Sci. Technol. 77 (2015) 675–687.
[55] H.N. Cuong, N.C. Minh, N. Van Hoa, T.S. Trung, Int. J. Biol. Macromol. 93 (2016) 442–447.
[56] J.R. Anusha, A.T. Fleming, Int. J. Biomater. 2016 (2016) 1–10.
[57] S. Palanisamy, M. Vinosha, M. Manikandakrishnan, R. Anjali, P. Rajasekar, T. Marudhupandi, R. Manikandan, B. Vaseeharan, N.M. Prabhu, Int. J. Biol. Macromol. 116 (2018) 151–161.
[58] A.F. Hifney, M.A. Fawzy, K.M. Abdel-Gawad, M. Gomaa, Food Hydrocoll. 54 (2016) 77–88.
[59] R. Artemisia, A.K. Nugroho, E.P. Setyowati, R. Martien, Indonesian J. Pharm. 30 (2019) 43–51.
[60] L. Xin, L. Bin, W. Xiao-Lei, S. Zhen-Liang, W. Chang-Yun, Czech J. Food Sci. 34 (2016) 406–413.
[61] T. Marudhupandi, T.T.A. Kumar, J. Coast. Life Med. 1 (2013) 282–286.
[62] C.-Y. Wang, Y.-C. Chen, J. Mar. Sci. Technol. 24 (2016) 319–328.
[63] A. Isnansetyo, F.N.Laili Lutfia, M. Nursid, T. T, R.A. Susidarti, Pharmacogn. J. 9 (2016) 14–20.
[64] W.F. Bahou, C.L. Potter, H. Mirza, Blood J. 84 (1994) 3734–3741.
[65] C.G. Knight, L.F. Morton, A.R. Peachey, D.S. Tuckwell, R.W. Farndale, M. J. Barnes, J. Biol. Chem. 275 (2000) 35–40.
[66] M.D. Shoulders, R.T. Raines, Annu. Rev. Biochem. 78 (2009) 929–958.
[67] S. Alkildani, O. Jung, M. Barceck, Anticancer Res. 41 (2021) 707/717.
[68] J. Zhang, R. Duan, L. Huang, Y. Song, J.M. Regenstein, Food Chem. 150 (2014) 22–27.
[69] Y.K. Lin, D.C. Liu, Food Chem. 99 (2006) 244–251.
[70] S.Y. Bak, S.W. Lee, C.H. Choi, H.W. Kim, Materials 11 (2018) 1–16.
[71] A. Alves, A. Marques, E. Martins, T. Silva, R. Reis, Cosmetics 4 (2017) 39–55.
[72] R. Berisio, L. Vitagliano, L. Mazzarella, A. Zagari, Protein Sci. 11 (2002) 262–270.
[73] Geneva, Switzerland, 2007, pp. 1–23.
[74] Spring, MD, USA, 2016.
[75] in: E.M.A.-S.M. Health (Ed.), 2019.
[76] United States Pharmacopeia: Rockville, MD, USA, 2012, pp. 1–137.
[77] R. Song, M. Murphy, C. Li, K. Ting, C. Soo, Z. Zheng, Drug Des. Devel. Ther. 12 (2018) 3117–3145.
[78] A. Gijpferich, Biomaterials 17 (1996) 103–114.
[79] S. Lyu, D. Untereker, Int. J. Mol. Sci. 10 (2009) 4033–4065.
[80] H.S. Azevedo, R.L. Reis, Understanding the enzymatic degradation of biodegradable polymers and stratagies to control their degradation rate, in: R. L. Reis, J.S. Roman (Eds.), Biodegradable Systems in Tissue Engineering and Regenerative Medicine, CRC Press, 2005, pp. 177–201.
[81] N. Price, L. Stevens, Fundamentals of enzymology, in: The Cell and Molecular Biology of Catalytic Proteins, 3th ed., 1999.
[82] L. Chung, D. Dinakarpandian, N. Yoshida, J.L. Lauer-Fields, G.B. Fields, R. Visse, H. Nagase, EMBO J. 23 (2004) 3020–3030.
[83] R. Stern, G. Kogan, M.J. Jedrzejas, L. Soltes, Biotechnol. Adv. 25 (2007) 537–557.
[84] T. Kaneiwa, S. Mizumoto, K. Sugahara, S. Yamada, Glycobiology 20 (2010) 300–309.
[85] A. Lončarević, M. Ivanković, A. Rogina, L. Ye, J. Tissue Repair Regen. 1 (2017) 12–22.
[86] J. Reith, A. Berking, C. Mayer, J. Bacteriol. 193 (2011) 5386–5392.
[87] A.A. Salmeán, C. Hervé, B. Jørgensen, W.G.T. Willats, J. Mravec, Front. Mar. Sci. 4 (2017) 1–8.
[88] N.L. Benbow, D.A. Sebben, S. Karpiniec, D. Stringer, M. Krasowska, D.A. Beattie, J. Colloid Interface Sci. 565 (2020) 555–566.
[89] J.H. Fitton, Mar. Drugs 9 (2011) 1731–1760.
[90] A. Gloria, A. Borzacchiello, F. Causa, L. Ambrosio, J. Biomater. Appl. 26 (2012) 745–759.
[91] J.M. Zuidema, C.J. Rivet, R.J. Gilbert, F.A. Morrison, J Biomed Mater Res B Appl Biomater 102 (2014) 1063–1073.
[92] A. Borzacchiello, L. Mayol, P.A. Ramires, A. Pastorello, C. Di Bartolo, L. Ambrosio, E. Milella, Biomaterials 28 (2007) 4399–4408.
[93] D. Fassini, A.R.C. Duarte, R.L. Reis, T.H. Silva, Mar. Drugs 15 (2017) 1–18.
[94] E. Perez-Herrero, P. Garcia-Garcia, J. Gomez-Morales, M. Llabres, A. Delgado, C. Evora, Regener. Biomater. 6 (2019) 149–162.
[95] L. Gao, Y. Zhou, J. Peng, C. Xu, Q. Xu, M. Xing, J. Chang, NPG Asia Mater. 11 (2019) 11–66.
[96] A. Citkowska, M. Szekalska, K. Winnicka, Mar. Drugs 17 (2019) 1–20.
[97] J.C. Suárez, Bioadhesives, in: Handbook of Adhesion Technology, 2011, pp. 1385–1408.
[98] I.O.f. Standardization (Ed.), ISO 10993-5, 2009.
[99] Y.E. Arslan, İ. Kantarcıoğlu, J. Turk. Chem. Soc. Sect. A Chem. (2019) 51–62.
[100] A. Bernhardt, B. Paul, M. Gelinsky, Mar. Drugs 16 (2018) 1–16.
[101] J. Garcia-Lopez, D. Garciadiego-Cazares, Y. Melgarejo-Ramirez, R. Sanchez-Sanchez, L. Solis-Arrieta, Z. Garcia-Carvajal, J.I. Sanchez-Betancourt, C. Ibarra, G. Luna-Barcenas, C. Velasquillo, Histol. Histopathol. 30 (2015) 1477–14785.
[102] X. Liang, X. Wang, Q. Xu, Y. Lu, Y. Zhang, H. Xia, A. Lu, L. Zhang, Biomacromolecules 19 (2018) 340–352.
[103] X. Wu, L. Black, G. Santacana-Laffitte, C.W. Patrick Jr., J. Biomed. Mater. Res. 81 (2007) 59–65.

Duarte Nuno Carvalho received his BSc (2015) and MSc (2017) degrees from the Polytechnic Institute of Leiria, ESTM, Portugal in Marine Research biotechnology. Currently, is getting a PhD (since 2018) in Tissue Engineering, Regenerative Medicine and Stem Cells from the University of Minho, Portugal. He has focused on developed innovative biomaterials based on marine origin polymers for cartilage biomedical approaches. He is author of 4 experimental scientific publications, 1 review, 1 book chapter and 1 patent.

David S. Williams, MChem MRSC CChem PhD is Head of Chemistry at Jellagen Ltd. David's expertise is in the development of novel materials based on natural and synthetic polymers. His publications in the areas of nanomedicine and biopolymer materials have spawned various new areas of research. He is now working to develop the next generation of soft technologies based on the unique properties of Collagen Type 0.

Carmen G. Sotelo PhD, she belongs to Seafood Biochemistry group in the Instituto de Investigaciones Marinas of CSIC. Carmen has worked in the isolation and characterization of collagen from different marine organisms. The main objective is to extract collagen from discarded species and/or fishery by-products to valorise it, developing new raw materials with application in different fields.

Ricardo I. Pérez-Martín PhD is Research Professor at the Institute of Marine Research (CSIC) in Vigo (Spain). He was Director of the Institute (1994–2001) and, at that time, he worked on the development of DNA-based techniques for the authentication of marine species in the control of food product labeling. He is now working, among other research lines, on obtaining useful compounds from fishery discards and by-products, such as collagen, chitosan or chondroitin sulfate, to be utilized for the development of biomaterials and also for the cosmetic industry. He is author of more than 150 publications and 3 patents.

Andrew Mearns-Spragg PhD, FRSB, FRSC, FRSA is Founder & Chief Scientific Officer of Jellagen Ltd. Mearns-Spragg is a scientific entrepreneur and marine biotechnology pioneer with a successful track record of growing venture backed technology businesses. Mearns-Spragg founded Jellagen in 2013, where he established in-house Collagen Type 0 standards and first data sets. He also built the first ISO13485:2016 certified manufacturing plant of Collagen Type 0 derived from jellyfish. He is a Fellow of the Royal Society of Chemistry and the Royal Society of Biology.

Rui L. **Reis**, PhD, DSc, Hon. Causa MD, Hon Causa PhD, FBSE, FTERM, member of NAE, FAIMBE, FEAMBES, is the Director of the 3B's Research Group - member of the I3Bs – Institute for Biomaterials, Biodegradables and Biomimetics, and the ICVS/3B's Associate Laboratory, both of UMinho. He is also the CEO of the European Institute of Excellence on Tissue Engineering and Regenerative Medicine (TERM), the Global Past-President of the TERM International Society (TERMIS) and the Editor-in-chief of the Journal of Tissue Engineering and Regenerative Medicine. He is a recognized world expert in the TERM and biomaterials fields with more 1500 publications, 90 patents, and most more.

Tiago H. Silva is Senior Researcher at 3B's Research Group, I3Bs Research Institute on Biomaterials, Biodegradables and Biomimetics, from University of Minho (Portugal), being coordinator of research on Marine Inspired Biomaterials. He his graduated in Chemistry (2001) and PhD in Chemistry (2006), both by Faculty of Sciences, University of Porto (Portugal). He has about 15 years of experience in valorization of marine resources and by-products and his research focus on the cross-talk between blue and red biotechnologies, by aiming the development of marine inspired biomaterials for regenerative medicine strategies and other advanced therapies, namely for cancer and diabetes.